

Femtosecond laser direct writing of gratings and waveguides in high quantum efficiency erbium-doped Baccarat glass

K C Vishnubhatla^{1,2,3,4}, S Venugopal Rao^{5,9}, R Sai Santosh Kumar¹,
R Osellame⁴, S N B Bhaktha^{2,3}, S Turrell⁶, A Chiappini³, A Chiasera³,
M Ferrari³, M Mattarelli², M Montagna², R Ramponi⁴, G C Righini^{7,8}
and D Narayana Rao^{1,9}

¹ School of Physics, University of Hyderabad, Hyderabad 500046, India

² Dipartimento di Fisica, CSMFO Lab., Università di Trento, 38050 Trento, Italy

³ CNR-IFN, CSMFO Lab., Via alla Cascata 56/c, 38050 Povo-Trento, Italy

⁴ IFN – CNR and Dipartimento di Fisica, Politecnico di Milano, Piazza Leonardo da Vinci, 32, 20133, Milano, Italy

⁵ ACRHEM, University of Hyderabad, Hyderabad 500046, India

⁶ Université des Sciences et Technologies de Lille, Laboratoire de Spectrochimie Infrarouge et Raman, Bâtiment C5 - UMR CNRS 8516, 59655 Villeneuve d'Ascq cedex, France

⁷ CNR-IFAC, MDF Lab., Sesto Fiorentino (Firenze), Italy

⁸ CNR, Department of Materials and Devices, via dei Taurini 19, 00185 Roma, Italy

E-mail: dnrsp@uohyd.ernet.in, svrsp@uohyd.ernet.in and krishna.vishunubhatla@polimi.it

Received 17 March 2009, in final form 7 September 2009

Published 25 September 2009

Online at stacks.iop.org/JPhysD/42/205106

Abstract

The femtosecond laser direct writing technique was employed to inscribe gratings and waveguides in high quantum efficiency erbium-doped Baccarat glass. Using the butt coupling technique, a systematic study of waveguide loss with respect to input pulse energy and writing speed was performed to achieve the best waveguide with low propagation loss (PL). By pumping at 980 nm, we observed signal enhancement in these active waveguides in the telecom spectral region. The refractive index change was smooth and we estimated it to be $\sim 10^{-3}$. The high quantum efficiency ($\sim 80\%$) and a best PL of ~ 0.9 dB cm⁻¹ combined with signal enhancement makes Baccarat glass a potential candidate for application in photonics.

(Some figures in this article are in colour only in the electronic version)

1. Introduction

During the last two decades there has been sustained interest in the development of erbium-doped gain amplifiers for the telecommunications spectral region [1, 2]. For achieving and realizing devices with optimized performance there has been consistent effort towards the development of host glass materials with superior spectroscopic properties. We have recently established the efficacy of erbium (Er) activated 'Baccarat' glass as a potential candidate for such applications [3, 4] and reported our initial results on laser direct writing of simple microstructures [5]. This modified silicate glass

has been produced at Cristallerie Baccarat by a conventional melt-quenching technique with a molar composition of 77.29 SiO₂ : 11.86 K₂O : 10.37 PbO : 0.48 Sb₂O₃ and 0.2 mol% of Er³⁺. Refractive index value at 1542 nm measured using the prism coupling method was 1.5427. Luminescence near 1.5 μ m was observed with a spectral width of ~ 18 nm. The decay curves of the ⁴I_{13/2} metastable state of the Er³⁺ ions presented a single exponential profile with a lifetime value of 14.2 ms. Using the Judd–Ofelt theory, quantum efficiency was estimated to be $\sim 80\%$. Such high quantum efficiency has been observed in Er³⁺-doped tellurite glasses but ours remains the highest amongst quantum efficiencies estimated in pure or modified-silica host glasses. To translate these spectroscopic

⁹ Author to whom any correspondence should be addressed.

advantages for practical device applications, fabrication of channel waveguides is essential. That the thresholds are lowered drastically in waveguide geometry, enabling the usage of low pump powers, further motivates the fabrication of waveguides in such materials.

Standard waveguide fabrication techniques consists of two main steps: (1) deposition of active glass material in the form of thin films onto substrates, e.g. pulsed laser deposition, RF sputtering, flame hydrolysis deposition, etc. (2) Inducing refractive index change (either into the thin films created by 1 or directly on the surface of glasses) by RIE, proton beam writing and other lithography based techniques [6, 7]. However, thin-film deposition is a rather complicated process and needs further efforts to obtain films with the same chemical composition and stoichiometry as that of the target [6]. Recent advances in femtosecond laser direct writing (FLDW) demonstrate unprecedented prospects for fabrication and rapid prototyping of highly functional photonic devices directly inside transparent dielectrics [8, 9]. FLDW has the proven ability to precisely induce refractive index change in a controlled fashion devoid of the material composition alteration. This ultrafast, multi-photon interaction does not require specially prepared or photosensitive materials. Moreover, the fabrication procedure is completed in a single step. Hence, this technique serves as a quick and proficient tool for fabrication of waveguides in materials not explored before, enabling rapid analysis and evaluation of novel active glasses and thereby develops active devices. It is now a well-established technique for fabrication of active and passive low-loss photonic components, micro-optics, fibre Bragg gratings, nanostructures, waveguide lasers, joining/welding of dissimilar glasses, lab-on-a-chip devices, etc [10–25]. In particular, this technique has the potential to develop erbium-doped waveguide amplifiers (EDWA) for metropolitan area network and local area network applications. Various active glasses including phosphates [26, 27], silicates [28, 29], tellurites [30, 31] and borates [32] have been investigated for writing active waveguides using this technique. Herein, we present the evaluation and performance of gratings and active waveguides inscribed in Baccarat glass using femtosecond pulses. For physical characterization of the modified zones absorption, emission and Raman spectroscopic techniques were employed.

2. Experimental details

For FLDW we employed ~ 100 femtosecond (fs) pulses from a Ti:sapphire amplifier (Mai-Tai, Spitfire) near 800 nm with 1 kHz repetition rate [5, 6]. The beam was focused into the sample using a microscope objective (MO) (typically $40\times$ with 0.65 NA) and writing was performed in the transverse geometry. The pulses used were nearly transform-limited which was ascertained from the time-bandwidth product. Appropriate neutral density filters were used to attenuate energy of the input beam. The problem of ellipticity of waveguides associated with transverse writing can be solved with (a) the use of telescopic lenses [33], (b) the use of a rectangular slit [26] or (c) using the multi-scan technique [28].

In the present case we employed a rectangular slit, which was inserted before the focusing objective. The slit width could be varied from 0.5 to 2.0 mm in steps of 0.5 mm. The slit modified the spatial profile of input beam and thereby the focal volume enabling us to achieve waveguides with circular cross-section. The sample was placed on a three-dimensional nano-positioner with <20 nm travel accuracy. The polarization of the input beam was perpendicular to the writing direction. Initially simple grating structures were written and the change in refractive index was estimated from the diffraction efficiency measurements.

3. Results

Figure 1(a) shows the confocal microscope image of a typical grating structure achieved with $20\ \mu\text{J}$ energy and a scanning speed of $50\ \mu\text{m s}^{-1}$. The inset of figure 1(a) depicts the diffraction pattern from a He-Ne laser. Several gratings were fabricated with varying energies and writing speeds. A best diffraction efficiency of $\sim 12\%$ (defined as the ratio of power diffracted into the first order to the input power) was accomplished from the grating written with an energy of $\sim 25\ \mu\text{J}$ and $500\ \mu\text{m s}^{-1}$ writing speed. This represents one of the highest diffraction efficiencies reported in gratings achieved in glasses with femtosecond pulses. From the diffraction efficiency measurements the change in the refractive index was estimated to be $\sim 2.2 \times 10^{-3}$ [5]. The periodicity and grating widths could be controlled through the input energy, writing speed and focal conditions. We achieved grating periods (and spacing) ranging from 4 to $10\ \mu\text{m}$. Later, about seventy single-line structures were written in the sample with varying energies ($1\text{--}90\ \mu\text{J}$), scan speeds ($250\ \mu\text{m s}^{-1}\text{--}2\ \text{mm s}^{-1}$) and slit widths ($0.5\text{--}1.5\ \text{mm}$) for identifying the optimized writing parameters to achieve smooth waveguides. Light was coupled into all of those structures to identify the actual waveguides. The grating structures were used for the micro-Raman spectroscopic studies to identify the physical mechanism responsible for the change in the index. The modified regions were investigated using the micro-Raman technique for an insight into the physical changes at the focus due to fsec pulses. Two main differences between the irradiated and the unirradiated regions were observed: (1) an increase in the sharp defect band at $596\ \text{cm}^{-1}$ and (2) an increase in intensity and line width of the broad band at about $470\ \text{cm}^{-1}$. This corresponds to a hardening of the structure by irradiation which can be associated with a positive refractive index change [34–37]. Figure 1(c) depicts the Raman mapping of the feature at $590\ \text{cm}^{-1}$. The top part is the optical image while the highlighted white rectangle indicates the region selected for mapping and the bottom part depicts the intensity mapping of the Raman peak at $590\ \text{cm}^{-1}$ suggesting periodic and smooth refractive index changes. Figures 1(d) and (e) illustrate the UV-visible and FTIR transmission behaviour of the modified and unmodified regions in the same sample. There are slight changes in the UV-visible spectra in the modified region while the FTIR spectra look identical for both the regions. The change in UV-visible transmittance could possibly result from

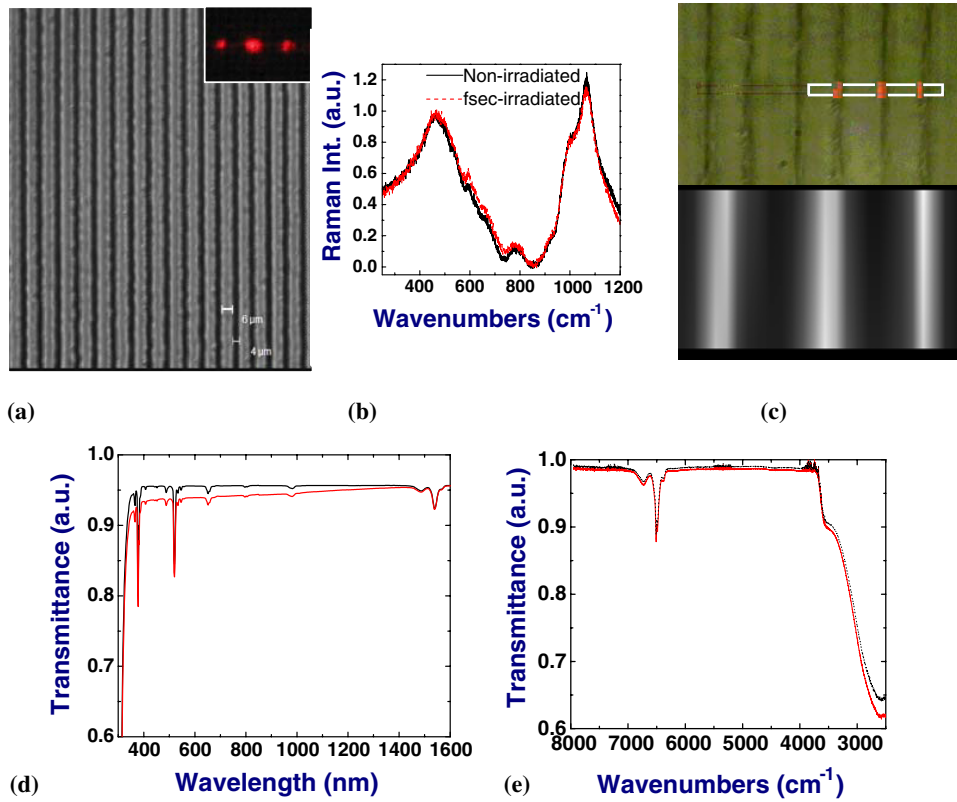


Figure 1. (a) Confocal microscopic image of a typical grating structure ($4\ \mu\text{m}$ width, $6\ \mu\text{m}$ period) inscribed in Baccarat; inset depicts the diffraction image from a He-Ne laser. (b) Micro-Raman spectra recorded from the modified (red/grey) and pristine region (black) of the glass. (c) Top part depicts the optical image of the grating inscribed into Baccarat glass; the white rectangular highlighted region was mapped for intensity. Bottom part shows the integrated intensity image of the Raman peak at $590\ \text{cm}^{-1}$ for three lines of the grating structure. Transmittance of modified (red/grey) and unmodified (black) regions of sample in (d) UV-visible and (e) FTIR spectral region. (Colour online.)

the diffraction/scattering of the incident light from grating-like structures in the spectrometer or manifestation of the modification itself which require further investigations.

Optical characterization of the waveguides was performed using a semiconductor tunable laser (ECL-200, Santec) at $1.6\ \mu\text{m}$ with a fibre coupled output. The light was butt-coupled into the waveguides. The radiation from the exit face of waveguides was collected with a $20\times$ objective and focused on a vidicon camera (C-2400, Hamamatsu) for capturing the near field profiles.

Figure 2(a) shows the mode profile from the coupling fibre whereas the mode profile of a waveguide written using a slit of $1.5\ \text{mm}$ is shown in figure 2(b) and without a slit is shown in figure 2(c). The writing parameters were constant (scanning speed: $500\ \mu\text{m s}^{-1}$, pulse energy: $30\ \mu\text{J}$) for figures 2(b) and (c) except for the presence of the slit. The effect of the slit is clearly visible in figure 2(b) with the mode profile being circular and is comparable to the fibre mode, while the waveguide profile without the slit is highly elliptical. Figure 3(a) depicts the mode profile obtained from the lowest loss waveguide ($0.5\ \text{mm}$ slit, $30\ \mu\text{J}$ energy and scanning speed of $50\ \mu\text{m s}^{-1}$), and the corresponding intensity distribution is illustrated in figure 3(b).

An important parameter to assess the quality of fabricated waveguides is the propagation loss (PL). The setup for waveguide loss measurement was similar to that of the mode

profile acquisition; the camera was replaced with a germanium detector to measure the power output from the waveguide P_{out} . Later the waveguide was removed and the fibre exit face was moved such that it was in the focus of the objective. The laser intensity from the fibre was measured, which gave the input power P_{in} . The total loss, TL, is given by

$$\text{TL} = -10 \log_{10} \frac{P_{\text{out}}}{P_{\text{in}}}. \quad (1)$$

Since the same microscope objective was used for measuring P_{out} and P_{in} , the losses in the collection end or the coupling end are common and eventually cancel out. Therefore, the TL in the waveguide is a sum of Fresnel loss (FL), coupling loss (CL) and the PL. The CL between the fibre and the waveguide was estimated from the extent of overlap of the fibre mode with that of the waveguide mode. By subtracting the values of CL and twice the FL (to compensate the loss from two facets of the waveguide) from the TL, the PL of the waveguides was obtained. Figure 4(a) shows the plot of the measured PL in dB cm^{-1} for waveguides fabricated with different scan speeds, pulse energies and slit widths. The following conclusions can be effectively drawn from the data presented. The slit width affects the spatial profile of the pulse at the focal volume and therefore the properties of waveguides. It is evident from figure 4(a) that the waveguides written using $0.5\ \text{mm}$ wide slit (circles) have lower losses compared with those written

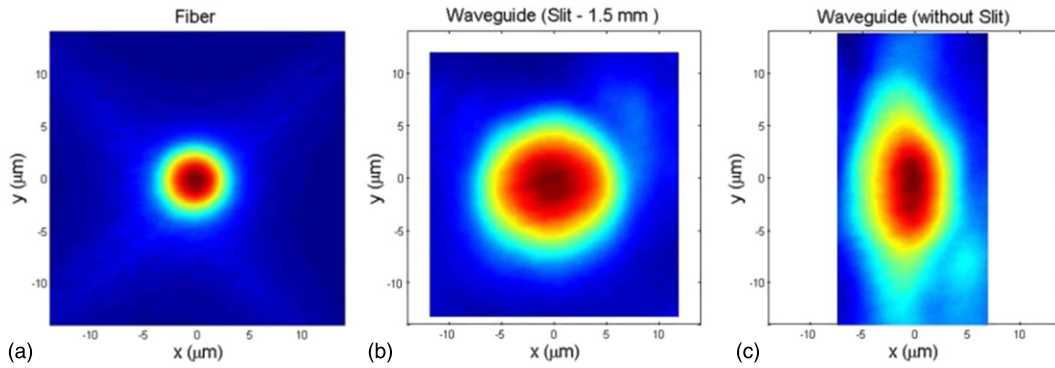


Figure 2. (a) The mode profile obtained with SMF 28 SMF. (b) The mode profile from using a slit. (c) The mode profile recorded for waveguide achieved without the slit. The scales on the x - and y -axis are from -10 to $10 \mu\text{m}$. (Colour online.)

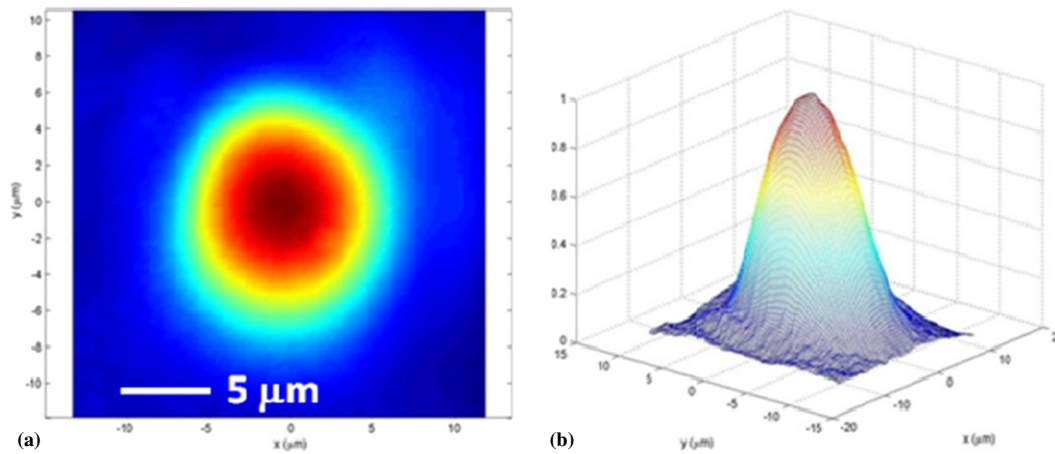


Figure 3. (a) The mode profile and (b) the intensity profile of the lowest loss waveguide achieved using 0.5 mm slit, $30 \mu\text{J}$ energy and scanning speed of $50 \mu\text{m s}^{-1}$. (Colour online.)

using 1.5 mm slit (triangles). The pulse energy determines whether the modification of the glass is in the damage regime or a uniform refractive index modification regime. At higher pulse energies the damage could create scattering points and voids along the waveguide. This will be highly unfavourable for waveguiding leading to high PLs. If the pulse energy is too low then the refractive index modification may not be sufficient enough for confinement, again leading to higher losses.

This is also apparent from the graph in figure 4(a), for any of the two slit widths, the waveguides written at $30 \mu\text{J}$ pulse energy have relatively low losses compared with the waveguides written with $85 \mu\text{J}$ pulse energy. Guiding was not observed in structures written with pulse energies $< 30 \mu\text{J}$. For pulse energies $> 85 \mu\text{J}$, we observed damage (probably void formation) leading to high PLs. For a given slit width and pulse energy, an optimal sample translation speed can be associated ($50 \mu\text{m s}^{-1}$ for circles and $250 \mu\text{m s}^{-1}$ for triangles), leading to a low-loss regime. At lower writing speeds, owing to the multiple exposure of the sample zone, the damage induced may be high, leading to high losses in the waveguides. At higher speeds due to lack of proper overlapping between the modified zones the confinement of the light may be poor, again leading to high losses. The energies presented here were estimated before the MO. Taking into account from the MO, errors in our power

meter calibration, errors in neutral density filter calibration we expect the actual energy values before it enters the sample to be less by at least 40%.

Taking into account estimated CL (estimated from the extent of overlap of fibre mode with that of the waveguide mode) of 0.7 dB and calculated FL of 0.2 dB , the PL of the waveguide written with optimal parameters (0.5 mm slit, $30 \mu\text{J}$ pulse energy, $50 \mu\text{m s}^{-1}$ scan speed) was estimated to be $< 0.9 \text{ dB cm}^{-1}$. An ideal system for the measurement of PLs would be the Fabry–Perot method or the scattering technique [38]. The losses predicted using our technique obviously has drawbacks and the values represented here are accurate within $\pm 15\%$. Obviously, these values need to be improved further and should be lowered to $< 0.2 \text{ dB cm}^{-1}$ for any practical device application and we expect to achieve this through either or combination of (a) the multiple scanning technique, (b) use of high repetition rate pulses [39], (c) use of longer pulses ($> 200 \text{ fs}$) and (d) isolating the optical table of any vibrations, which affects the smoothness of the waveguide. Nonetheless, this value compares reasonably well with those reported recently with Nandi *et al* [30] demonstrating $\sim 2 \text{ dB cm}^{-1}$ PLs in tellurite glasses and Bhardwaj *et al* [12] reporting $\leq 1 \text{ dB cm}^{-1}$ for several multi-component glasses.

Signal enhancement is an important figure of merit for the device to function as an amplifier. The 10 mm long

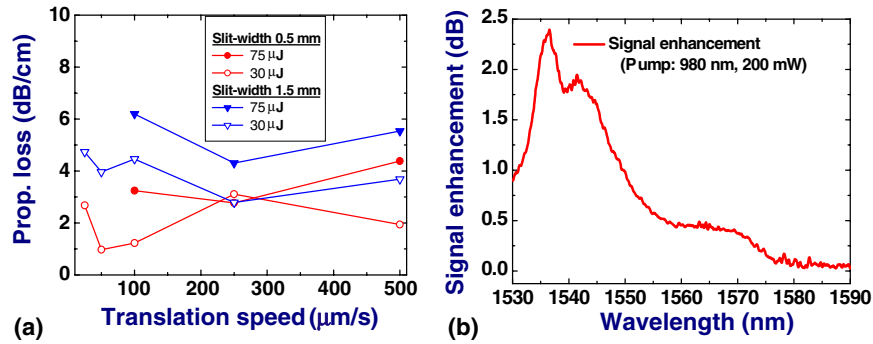


Figure 4. (a) Waveguide PLs obtained versus translation speed. (b) Signal enhancement obtained in the best waveguide with pumping at 980 nm.

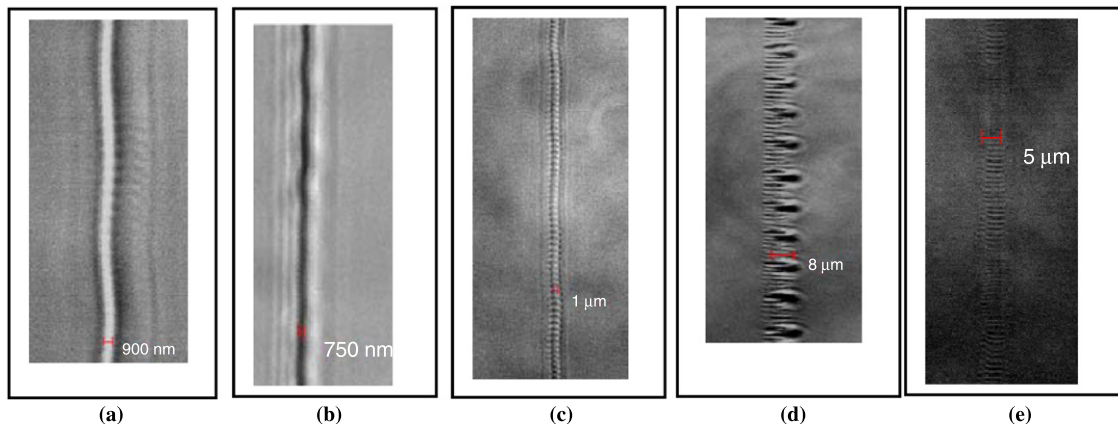


Figure 5. (a) 900 nm structure obtained with 1.5 mm slit, $<10 \mu\text{J}$ energy, $100 \mu\text{m s}^{-1}$ speed. (b) 750 nm wide structure obtained with 1.5 mm slit, $\sim 80 \mu\text{J}$ energy, $500 \mu\text{m s}^{-1}$ speed. (c) Pearl-chain-like structures obtained with 2.0 mm slit, $<5 \mu\text{J}$ energy, $100 \mu\text{m s}^{-1}$ speed. Bragg-grating-like structures acquired with (d) 0.5 mm slit, $<5 \mu\text{J}$ energy, $25 \mu\text{m s}^{-1}$ speed and (e) 0.5 mm slit, $<5 \mu\text{J}$ energy, $100 \mu\text{m s}^{-1}$ speed. Scale bars are 900 nm, 750 nm, 1 μm , 8 μm and 5 μm in (a), (b), (c), (d) and (e), respectively.

active waveguide (with the lowest PL) was butt-coupled on both sides to standard telecom single mode fibres (SMFs) using an index-matching fluid. A 980 nm wavelength InGaAs laser diode was used, which supplied $\sim 250 \text{ mW}$ incident pump power through 980/1550 nm wavelength-division-multiplexers (WDMs). Signal radiation in the telecom C-Band (1530–1565 nm) was provided by a broad band source, properly attenuated to about -3 dBm over a 100 nm bandwidth. The small signal enhancement of the amplifier as a function of wavelength, measured with an accuracy of about 0.5 dB with a pump power level of 200 mW, is shown in figure 4(b).

A signal enhancement of $\sim 2.3 \text{ dB}$ was observed at 1536 nm. However, the absorption and insertion losses had a peak at the same wavelength with a magnitude of $\sim 5.5 \text{ dB}$, implying the signal enhancement is insufficient to compensate for the losses. The main reason identified for this is lack of ytterbium co-doping in the sample which strongly limited the pumping efficiency. Nevertheless, these results reveal the possibility to fabricate low-loss waveguides in Baccarat with the LDW technique while preserving the active nature of erbium ions.

Apart from the waveguides, we observed some interesting characteristics in some of our structures, which could potentially be useful for other applications. Figures 5(a)–(e) depict the confocal microscope images of such structures

obtained with different writing conditions. Figures 5(a) and (b) demonstrate sub-micrometre wide structures written with (a) 1.5 mm slit, $<10 \mu\text{J}$ energy and $100 \mu\text{m s}^{-1}$ speed, (b) 1.5 mm slit, $\sim 80 \mu\text{J}$ energy and $500 \mu\text{m s}^{-1}$ speed. In the former case the energy used was less with slow scan speed while in the latter case high energy with faster scan speed was utilized and the effect was similar in both cases producing structures $<1 \mu\text{m}$ side. Similarly, figure 5(c) shows the pearl chain shaped structure [40] obtained using a 2.0 mm slit, $<5 \mu\text{J}$ energy and $100 \mu\text{m s}^{-1}$ scanning speed. Figures 5(d) and 4(e) illustrate Bragg-like structures acquired with (d) 0.5 mm slit, $<5 \mu\text{J}$ energy, $25 \mu\text{m s}^{-1}$ speed and (e) 0.5 mm slit, $<5 \mu\text{J}$ energy, $100 \mu\text{m s}^{-1}$ speed, respectively. The periodicity calculated from the structure in figure 4(e) was of the order of wavelength ($\sim 800 \text{ nm}$). The manifestation of such structures has been attributed to either (a) interference of the incident laser beam and the surface scattered waves, (b) the incident laser field interfering with the electron plasma wave proposed by Yang *et al* [23] and (c) the local field enhancement occurring during inhomogeneous broadening proposed by Bhardwaj *et al* [24]. In our case these structures need further detailed investigations including energy and polarization dependence to completely understand the origin. However, the appearance of such structures again demonstrates the capabilities of the LDW technique to fabricate several optical components, leading to

integration of active and passive devices, on a single substrate for photonic applications.

In conclusion, waveguiding was demonstrated in the structures written in Baccarat glasses using femtosecond laser pulses. With optimization of parameters such as slit width, scan speeds and pulse energies, PL of $<0.9 \text{ dB cm}^{-1}$ in the best waveguide was achieved. A signal enhancement of 2.3 dB was also observed at 1536 nm when pumped with 200 mW at 980 nm. A significant improvement in the gain performance is expected after co-doping with ytterbium. Our further studies will focus on (a) improving the PLs and (b) achieving ytterbium doping for gain purposes. Er-activated Baccarat glass, with its high quantum efficiency and the ease of fabricating low-loss waveguides with FLDW, stands as a promising glass for application in photonics.

Acknowledgments

S V Rao and D N Rao acknowledge the financial support from the DST, India, through SERC project SR/S2/LOP-11/2005. S V Rao acknowledges partial financial support from the ACRHEM, University of Hyderabad. KCV acknowledges the financial support from the 'India-Trento Program for Advanced Research' Phase II (2008-2011) research project and the Italian Ministry of University and Research for the scholarship grant. R S S Kumar acknowledges the financial support of the CSIR.

References

- [1] Miniscalco W J 1991 Erbium-doped glasses for fiber amplifiers at 1500 nm *J. Light. Technol.* **9** 234–50
- [2] Kenyon A J 2002 Recent developments in rare-earth doped materials for optoelectronics *Prog. Quantum Electron.* **26** 225–84
- [3] Bhaktha S N B *et al* 2006 Erbium-activated modified silica glasses with high $^4\text{I}_{13/2}$ luminescence quantum yield *Opt. Mater.* **28** 1325–8
- [4] Vishnubhatla K C 2008 *PhD Thesis* University of Hyderabad, India and University of Trento, Italy
- [5] Vishnubhatla K C *et al* 2008 Micro-Raman mapping of micro-gratings in 'BACCARAT' glass directly written using femtosecond laser *Proc. SPIE* **6881** 688114
- [6] Pollnau M and Romanyuk Y E 2007 Optical waveguides in laser crystals *C.R. Physique* **8** 123–37
- [7] Bettiol A A, Venugopal Rao S and Watt F 2006 Fabrication of buried, channel waveguides in Foturan glass using proton beam writing *Appl. Phys. Lett.* **88** 171106
- [8] Davis K M, Miura K, Sugimoto N and Hirao K 1996 Writing waveguides in glass with a femtosecond laser *Opt. Lett.* **21** 1729–31
- [9] Gattass R R and Mazur E 2008 Femtosecond laser micromachining in transparent materials *Nature Photon.* **2** 219
- [10] Nolte S, Will M, Burghoff J and Tünnermann A 2003 Femtosecond waveguide writing a new avenue to three dimensional integrated optics *Appl. Phys. A* **77** 109–11
- [11] Cheng Y, Sugioka K, Masuda M, Shihoyama K, Toyoda K and Midorikawa K 2003 Optical gratings embedded in photosensitive glass by photochemical reaction using a femtosecond laser *Opt. Express* **11** 1809
- [12] Bhardwaj V R, Simova E, Corkum P B, Rayner D M, Hnatovsky C, Taylor R S, Schreder B, Kluge M and Zimmer J 2005 Femtosecond laser-induced refractive index modification in multicomponent glasses *J. Appl. Phys.* **97** 083102
- [13] Taccheo S *et al* 2004 Er: Yb-doped waveguide laser fabricated by femtosecond laser pulses *Opt. Lett.* **29** 2626–8
- [14] Cheng Y, Sugioka K and Midorikawa K 2003 Control of the cross-sectional shape of a hollow microchannel embedded in photostructurable glass by use of a femtosecond laser *Opt. Lett.* **28** 55–7
- [15] Tokuda Y, Saito M, Takahashi M, Yamada K, Watanabe W, Itoh K and Yoko T 2003 Waveguide formation in niobium tellurite glasses by pico- and femtosecond laser pulses *J. Non-Crystal. Solids* **326** 472–5
- [16] Cheng Y, Sugioka K and Midorikawa K 2004 Microfluidic laser embedded in glass by three-dimensional femtosecond laser microprocessing *Opt. Lett.* **29** 2007
- [17] Cheng Y, Sugioka K, Midorikawa K, Masuda M, Toyoda K, Kawachi M and Shihoyama K 2003 Three dimensional microoptical components embedded in photosensitive glass by a femtosecond laser *Opt. Lett.* **28** 1144–6
- [18] Shah L, Arai A Y, Eaton S M and Herman P R 2005 Waveguide writing in fused silica with a femtosecond fiber laser at 522 nm and 1 MHz repetition rate *Opt. Express* **13** 1999
- [19] Della Valle G, Osellame R, Chiodo N, Taccheo S, Cerullo G, Laporta P, Killi A, Morgner U, Lederer M and Kopf D 2005 C-band waveguide amplifier produced by femtosecond laser writing *Opt. Express* **13** 5976
- [20] Marshall G D, Dekker P, Ams M, Piper J A and Withford M J 2008 Directly written monolithic waveguide laser incorporating a distributed feedback waveguide-Bragg grating *Opt. Lett.* **33** 9
- [21] Tamaki T, Watanabe W and Itoh K 2006 Laser micro-welding of transparent materials by a localized heat accumulation effect using a femtosecond fiber laser at 1558 nm *Opt. Express* **14** 10460–8
- [22] Shimotsuma Y, Kazansky P G, Qiu J R and Hirao K 2003 Self-organized nanogratings in glass irradiated by ultrashort light pulses *Phys. Rev. Lett.* **91** 247405
- [23] Yang W, Bricchi E, Kazansky P G, Bovatsek J and Arai A Y 2006 Self-assembled periodic sub-wavelength structures by femtosecond laser direct writing *Opt. Express* **14** 10117–24
- [24] Bhardwaj V R, Simova E, Rajeev P P, Hnatovsky C, Taylor R S, Rayner D M and Corkum P B 2006 Optically produced arrays of planar nanostructures inside fused silica *Phys. Rev. Lett.* **96** 057404
- [25] Yang W J, Kazansky P G and Svirko Y P 2008 Non-reciprocal ultrafast laser writing *Nature Photon.* **2** 99–104
- [26] Ams M, Marshall G, Spence D and Withford M 2005 Slit beam shaping method for femtosecond laser direct-write fabrication of symmetric waveguides in bulk glasses *Opt. Express* **13** 5676
- [27] Chan J W, Huser T R, Risbud S H, Hayden J S and Krol D M 2003 Waveguide fabrication in phosphate glasses using femtosecond laser pulses *Appl. Phys. Lett.* **82** 2371–3
- [28] Psaila N D, Thomson R R, Bookey H T, Kar A K, Chiodo N, Osellame R, Cerullo G, Jha A and Shen S 2007 Er: Yb-doped oxyfluoride silicate glass waveguide amplifier fabricated using femtosecond laser inscription *Appl. Phys. Lett.* **90** 131102
- [29] Thomson R R, Campell S, Blewett I J, Kar A K, Reid D T, Shen S and Jha A 2005 Active waveguide fabrication in erbium-doped oxyfluoride silicate glass using femtosecond pulses *Appl. Phys. Lett.* **87** 121102
- [30] Nandi P, Jose G, Jayakrishnan C, Debbarma S, Chalapathi K, Aleti K, Dharmadhikari A K, Dharmadhikari J A and Mathur D 2006 Femtosecond laser written channel waveguides in tellurite glass *Opt. Express* **14** 12145
- [31] Fernandez T T, Della Valle G, Osellame R, Jose G, Chiodo N, Jha A and Laporta P 2008 Active waveguides written by

- femtosecond laser irradiation in an erbium-doped phospho-tellurite glass *Opt. Express* **16** 15198–205
- [32] Yang W, Corbari C, Kazansky P G, Sakaguchi K and Carvalho I C 2008 Low loss photonic components in high index bismuth borate glass by femtosecond laser direct writing *Opt. Express* **16** 16215–26
- [33] Osellame R, Taccheo S, Marangoni M, Ramponi R, Laporta P, Polli D, De Silvestri S and Cerullo G 2003 Femtosecond writing of active optical waveguides with astigmatically shaped beams *J. Opt. Soc. Am. B* **20** 1559
- [34] Chan J W, Huster T R, Risbud S H and Krol D M 2003 Modification of the fused silica glass network associated with waveguide fabrication using femtosecond laser pulses *Appl. Phys. A* **76** 367–72
- [35] Chan J W, Huser T, Risbud S and Krol D 2001 Structural changes in fused silica after exposure to focused femtosecond laser pulses *Opt. Lett.* **26** 1726–8
- [36] Reichman W J, Krol D M, Shah L, Yoshino F, Arai A, Eaton S M and Herman P R 2006 A spectroscopic comparison of femtosecond-laser-modified fused silica using kilohertz and megahertz laser systems *J. Appl. Phys.* **99** 123112
- [37] Reichman W, Chan J W and Krol D M 2003 Confocal fluorescence and Raman microscopy of femtosecond laser-modified fused silica *J. Phys.: Condens. Matter* **15** S2447–456
- [38] Venugopal Rao S, Moutzouris K, Ebrahimzadeh M, De Rossi A, Calligaro M, Ortiz V, Ginitz G and Berger V 2002 Measurements of optical loss in GaAs/Al₂O₃ nonlinear waveguides in the infrared using femtosecond scattering technique *Opt. Commun.* **213** 223–8
- [39] Eaton S, Zhang H, Herman P, Yoshino F, Shah L, Bovatsek J and Arai A 2005 Heat accumulation effects in femtosecond laser-written waveguides with variable repetition rate *Opt. Express* **13** 4708–16
- [40] Graf R, Fernandez A, Dubov M, Brueckner H J, Chichkov B N and Apolonski A 2007 Pearl-chain waveguides written at megahertz repetition rate *Appl. Phys. B* **87** 21–7